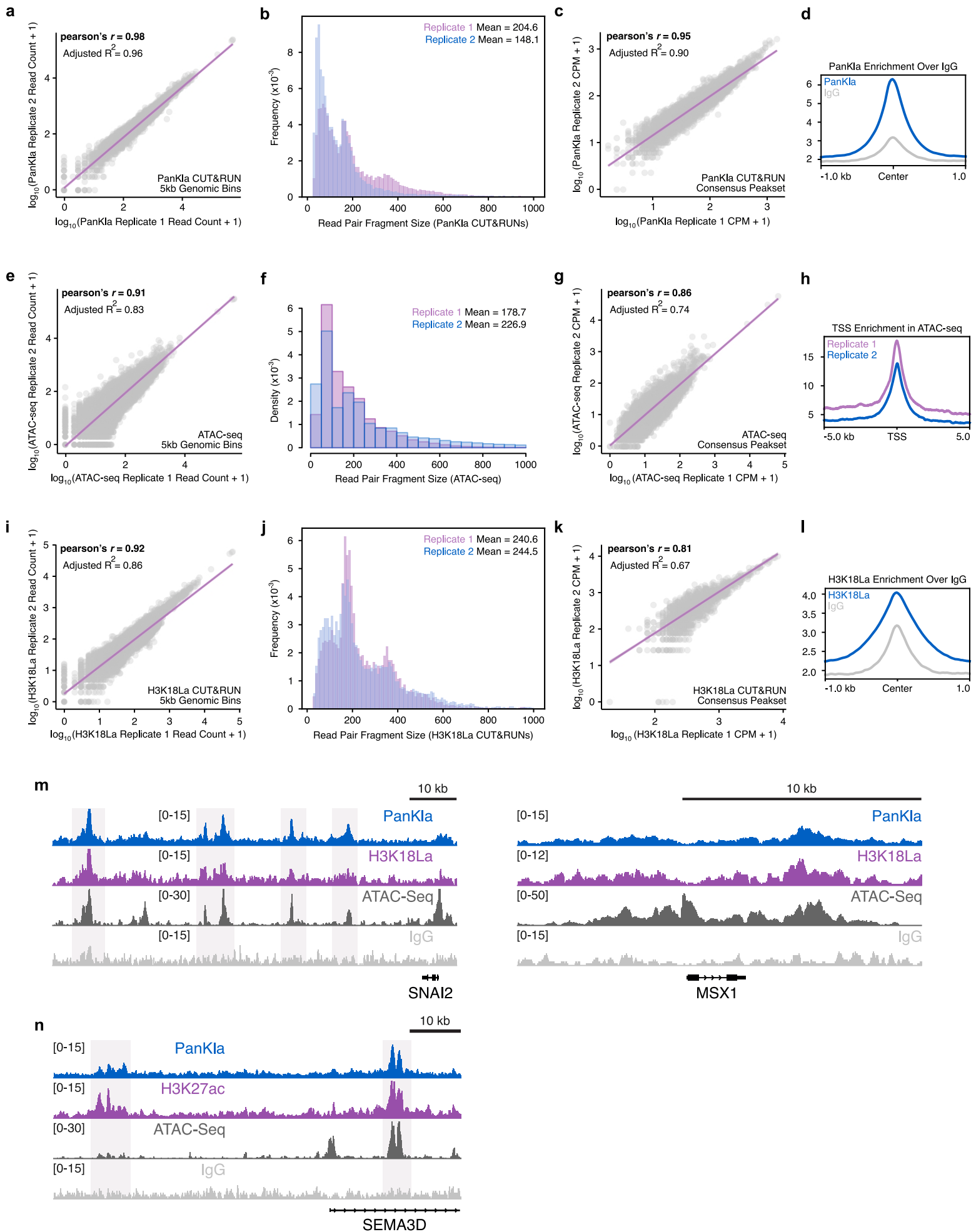


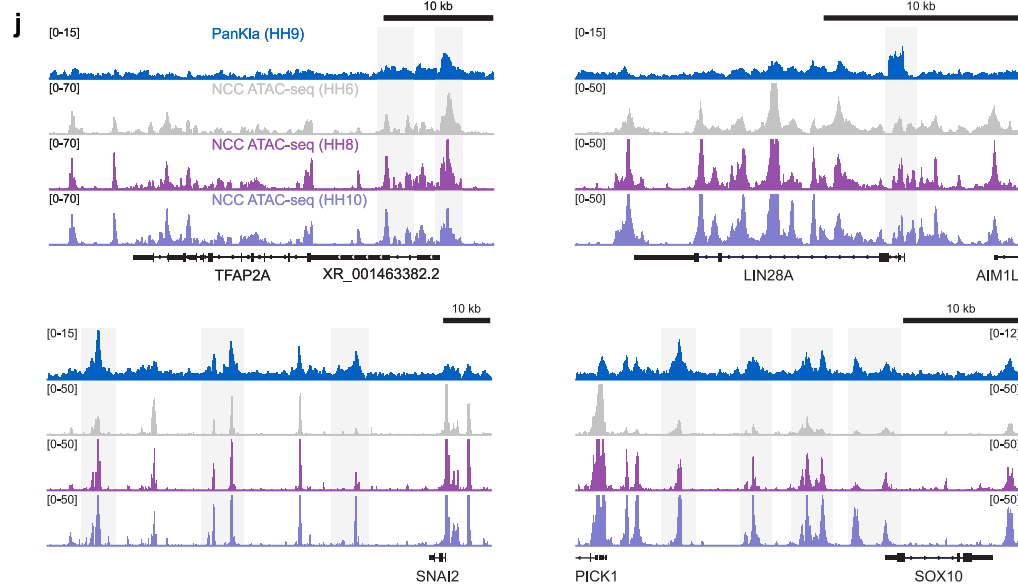
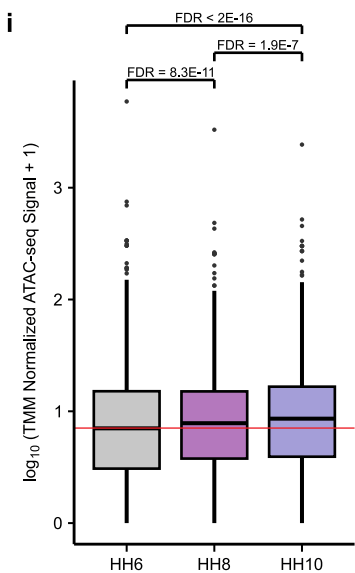
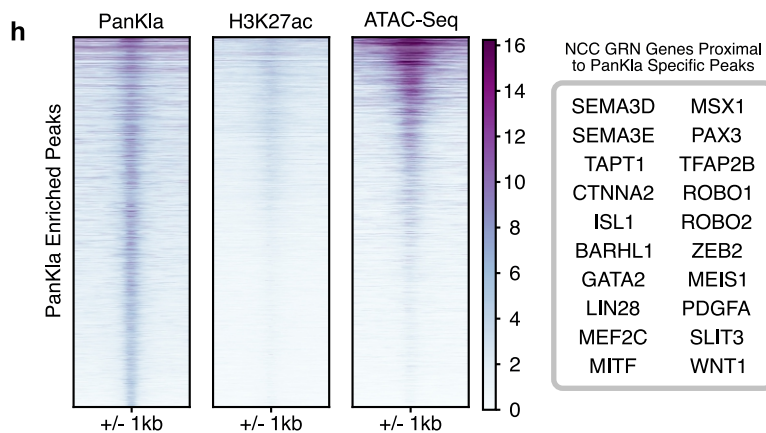
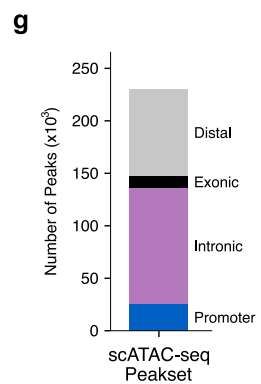
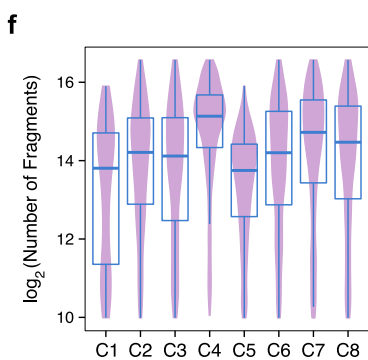
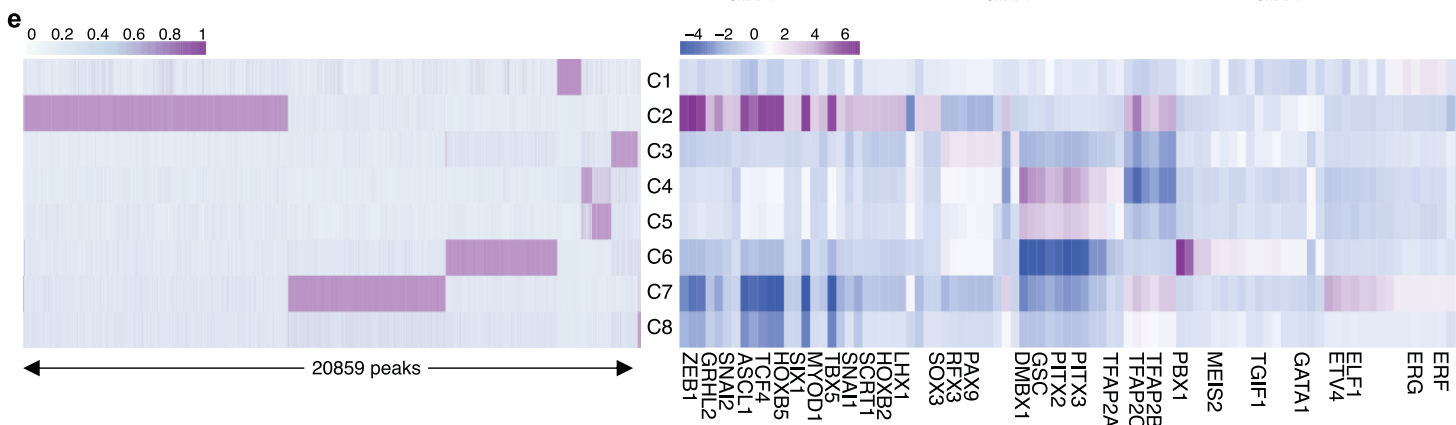
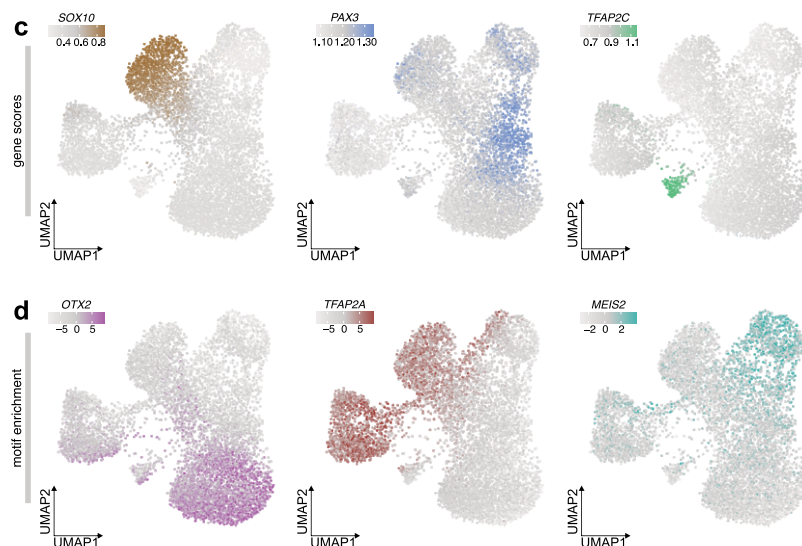
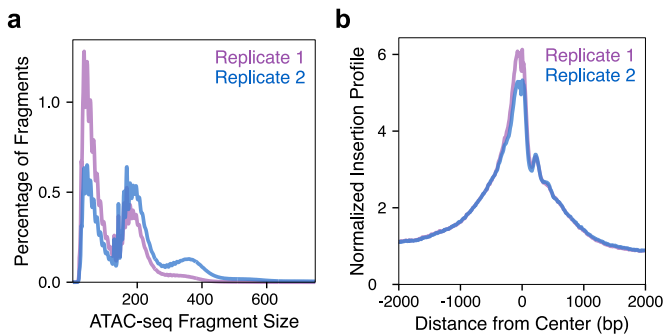
Supplementary Figure 1 – Flow cytometry gating strategy and control plots for lactylation level quantification experiment.

(A-C) Contour plots showing the relative density of events in subsequent gating steps for cell samples stained only with secondary antibodies (Alexa647 and Alexa488). Gates are displayed as colored lines and the percentage/number of events in the gate is shown. Fluorescent intensity gates (C) are used for all of the following samples to define specific populations. (D-F) Contour plots showing the relative density of events in subsequent gating steps for HH6 samples stained with PAX7 (Alexa488) and PanKla (Alexa647) antibodies. Gates are displayed as colored lines and the percentage/number of events in the gate is displayed. (G-I) Contour plots showing the relative density of events in subsequent gating steps for HH9 samples stained with TFAP2B (Alexa488) and PanKla (Alexa647) antibodies. Gates are displayed as colored lines and the percentage/number of events in the gate is shown. (J-L) Contour plots showing the relative density of events in subsequent gating steps for HH12-13 samples stained with TFAP2B (Alexa488) and PanKla (Alexa647) antibodies. Gates are displayed as colored lines and the percentage/number of events in the gate is shown. (M) Histograms of lactylation levels (Alexa647-A) for cells in the purple (F), blue (I), and gray (L) gates defining PAX7+ NPBCs, TFAP2B+ pre-migratory/delaminating NCCs, and TFAP2B+ migratory NCCs respectively. The percentage of cells in the gate defined by the black lines is displayed. (N) Dot plot showing the median of the distribution of lactylation levels for the cells in the purple (F), blue (I), and gray (L) gates for both biological replicates.



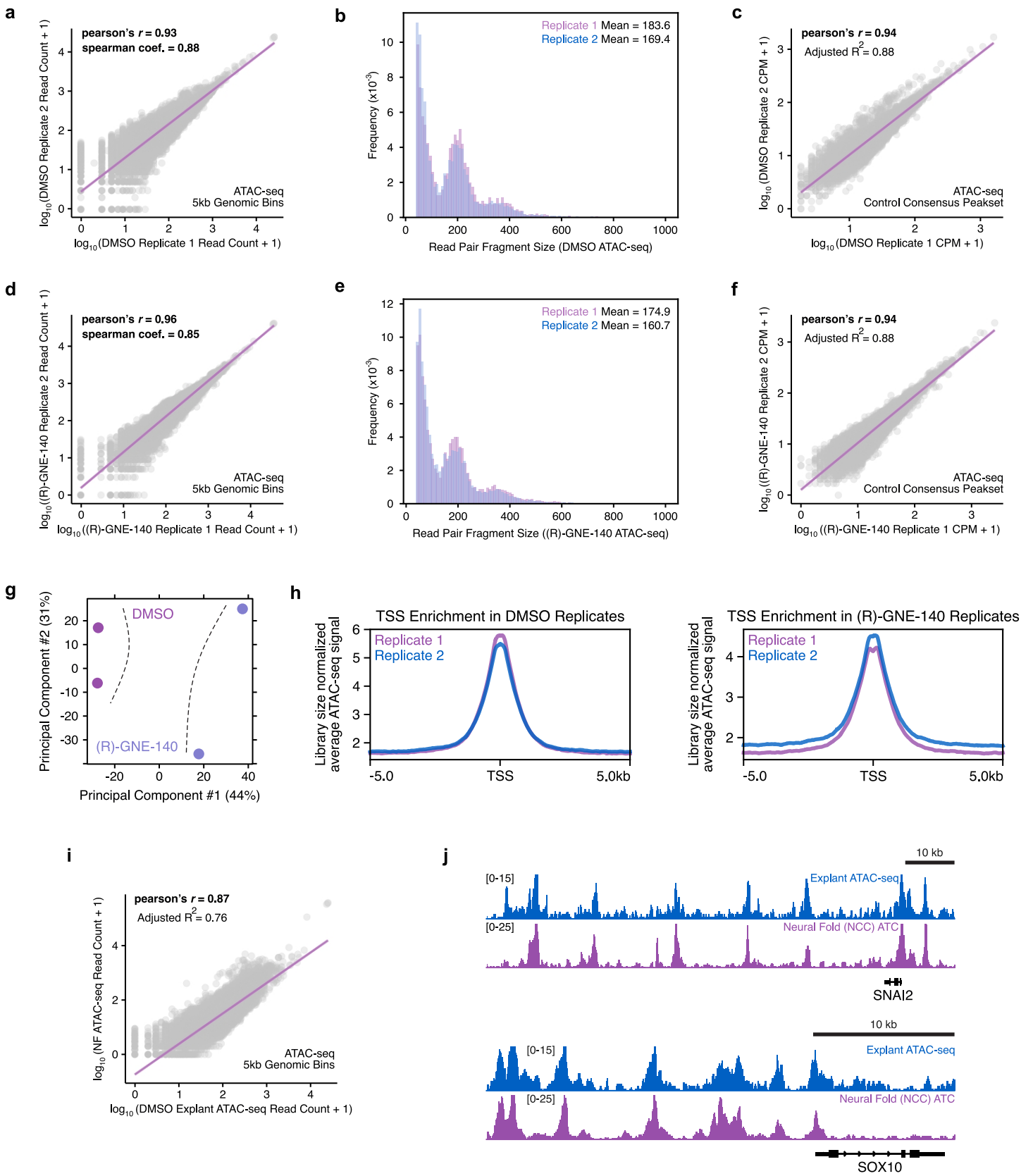
Supplementary Figure 2 – Quality control metrics for PanKla and H3K18La CUT&RUN as well as neural fold ATAC-seq datasets.

(A) Scatterplot of read count from each PanKla replicate CUT&RUN alignment file at regions obtained after binning the genome into 5kb fragments (213380 bins). Magenta line is the line of best fit from regression analysis. (B) Overlaid histograms of read pair fragment size distribution for both PanKla CUT&RUN replicates. (C) Scatter plot of sequencing depth normalized PanKla signal from each replicate at consensus PanKla peakset (10612 peaks). (D) Profile plot showing cumulative PanKla and IgG signal at PanKla consensus peakset. PanKla signal displayed as average between replicates. (E) Scatterplot of read count from each neural fold ATAC-seq replicate alignment file at regions obtained after binning the genome into 5kb fragments (213312 bins). Magenta line is the line of best fit from regression analysis. (F) Overlaid histograms of read pair fragment size distribution for both ATAC-seq replicates. (G) Scatter plot of sequencing depth normalized PanKla signal from each replicate at consensus PanKla peakset (38250 peaks). (H) Profile plots showing enrichment of ATAC-seq signal at transcription start sites (TSS) for both replicates of each sample. (I) Scatterplot of read count from each H3K18La replicate CUT&RUN alignment file at regions obtained after binning the genome into 5kb fragments (213311 bins). Magenta line is the line of best fit from regression analysis. (J) Overlaid histograms of read pair fragment size distribution for both H3K18La CUT&RUN replicates. (K) Scatter plot of sequencing depth normalized H3K18La signal from each replicate at consensus H3K18La peakset (1578 peaks). (L) Profile plot showing cumulative H3K18La and IgG signal at H3K18La consensus peakset. H3K18La signal displayed as average between replicates. (M) Genome browser tracks showing PanKla CUT&RUN, H3K18La CUT&RUN, and ATAC-seq peaks at the SNAI2 and MSX1 loci. IgG track included as a control. (N) Genome browser tracks showing PanKla CUT&RUN, H3K27ac CUT&RUN, and ATAC-seq peaks at the SEMA3D locus. IgG track included as a control. RefSeq gene annotation tracks are used to visualize genes in genome browser panels. Non-curated non-coding RNA annotations are not displayed.



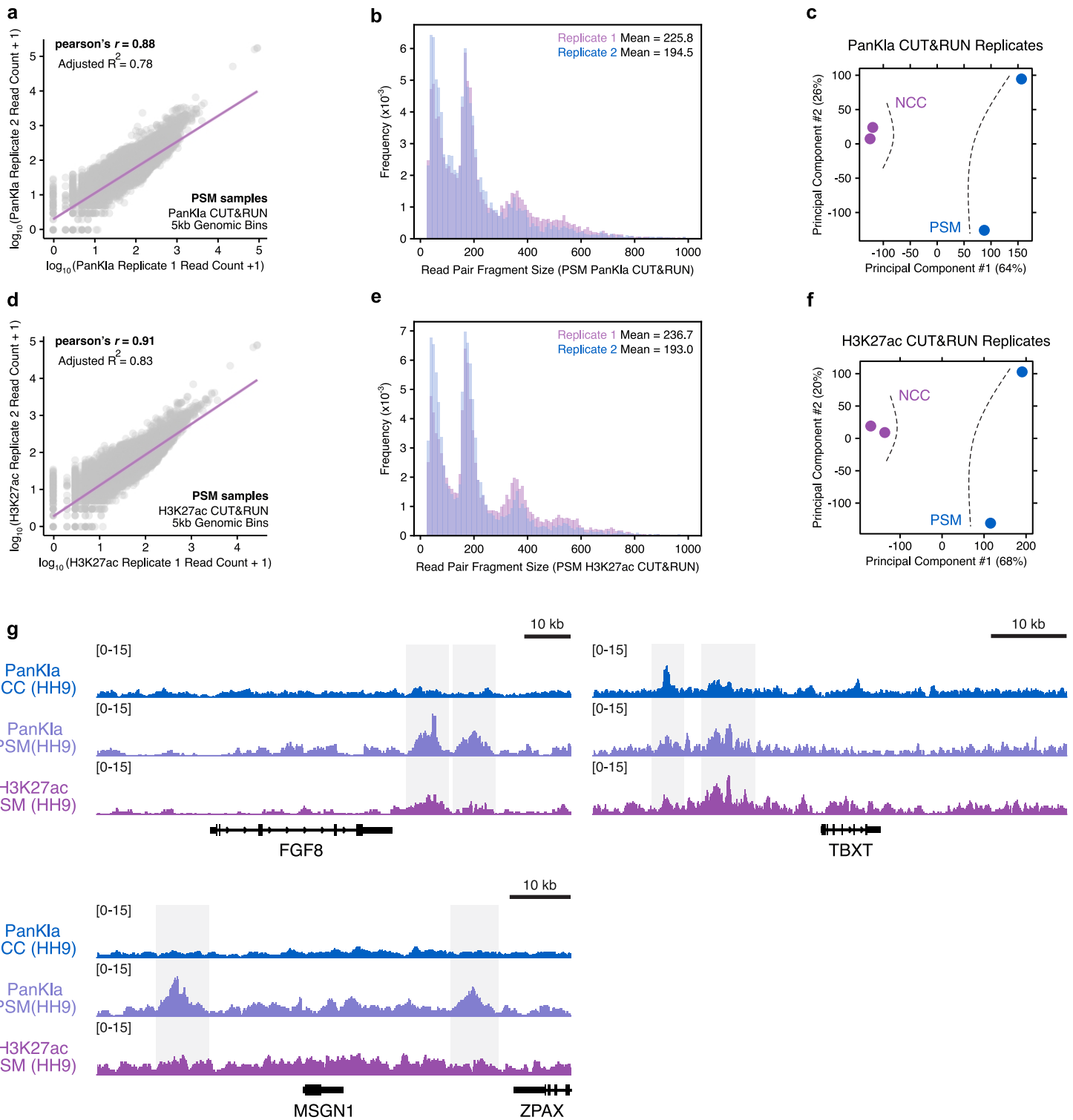
Supplementary Figure 3 – Quality control metrics and peak calling parameters for scATAC-seq dataset.

(A) Fragment size distribution of biological replicates from the scATAC-seq dataset showing nucleosomal binding pattern. (B) Profile plots showing enrichment of signal at transcription start sites (TSS) for both replicates of the scATAC-seq dataset. (C) ScATAC-seq UMAPs showing the projection of genescores for the transcription factors Sox10, Pax3, and Tfp2c. (D) ScATAC-seq UMAPs showing the motif enrichment projection for transcription factors Otx2, Tfp2a, and Meis2. (E) Heatmaps showing the significantly enriched peaks ($FDR < 0.1$, $\log_2FC > 2$) and associated top enriched motifs across the scATAC-seq clusters. (F) Violin plots showing the distribution of unique nuclear fragments per cells after filtering at each cluster in the scATAC-seq dataset. (G) Stacked barplot showing the genomic distribution of called peaks in the scATAC-seq dataset. (H) Tornado plots showing PanKla, H3K27ac, and bulk ATAC-seq signal at lactylation-enriched peaks used for projection onto the scATAC-seq UMAP in Figure 3C. Box to the right shows the NCC GRN genes that are associated with said lactylation-enriched peaks. (I) Boxplot of TMM normalized ATAC-seq signal at lactylated peaks (from the aggregate ATAC peakset) at three developmental stages. Kruskal-Wallis test ($\chi^2 = 128.51$, $df = 2$, $p\text{-value} = 1.244058E-28$), followed by *ad hoc* pairwise Wilcoxon rank sum test ($n_{HH6} = 10018$ peaks, $n_{HH8} = 10018$ peaks, $n_{HH10} = 10018$ peaks). The p -value was corrected for multiple comparisons using FDR (HH6 vs HH8 $p\text{-value} = 8.328737E-11$, HH8 vs HH10 $p\text{-value} = 1.885227E-07$, HH6 vs HH10 $p\text{-value} = 4.637372E-28$). Boxplot center line is median, box limits are upper and lower quartiles, whiskers are the 1.5X interquartile range, and individual points are outliers. (J) Genome browser tracks showing replicate average ATAC-seq signal from HH6, HH8, and HH10 NCC samples as well as HH9 PanKla at the TFAP2A, LIN28A, SNAI2, and SOX10 genomic loci. RefSeq gene annotation tracks are used to visualize genes in genome browser panels. Non-curated non-coding RNA annotations are not displayed for LIN28A, SNAI2, and SOX10 genomic loci.



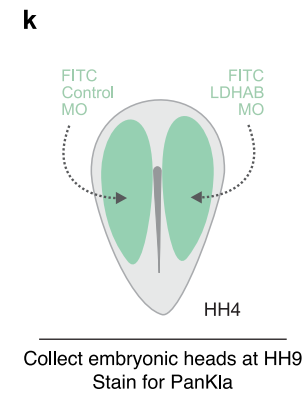
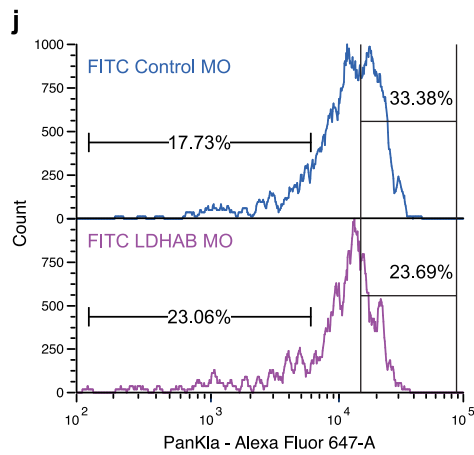
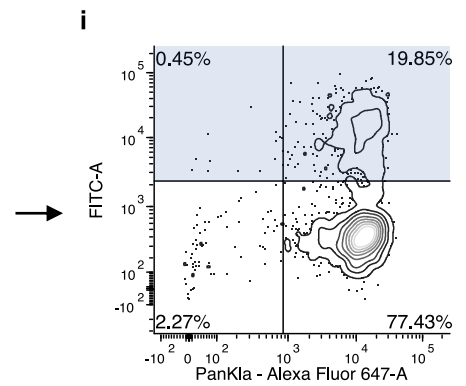
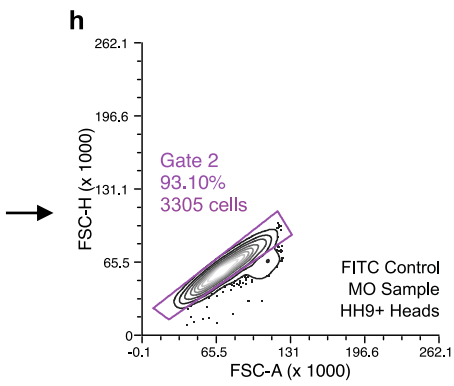
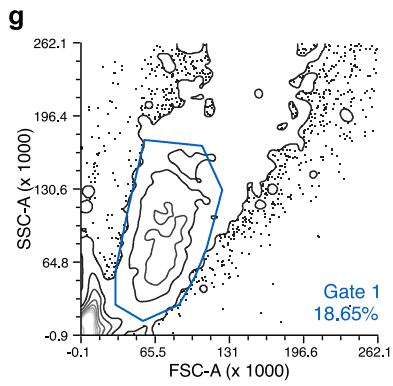
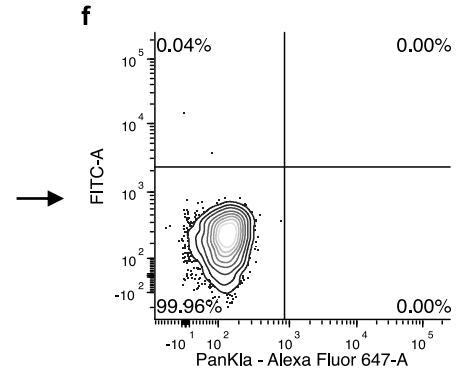
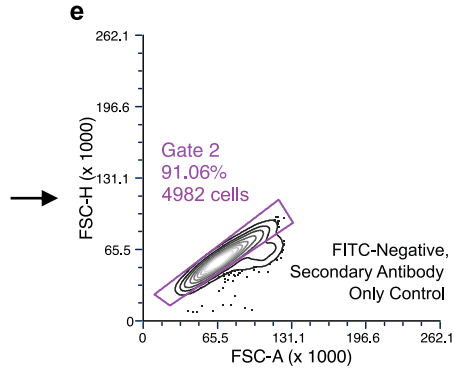
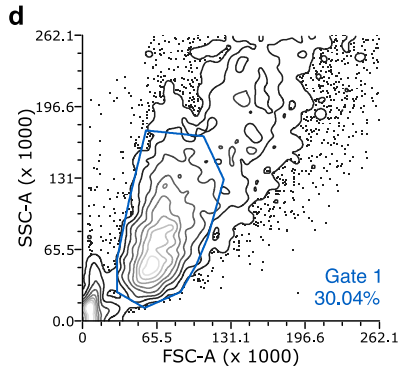
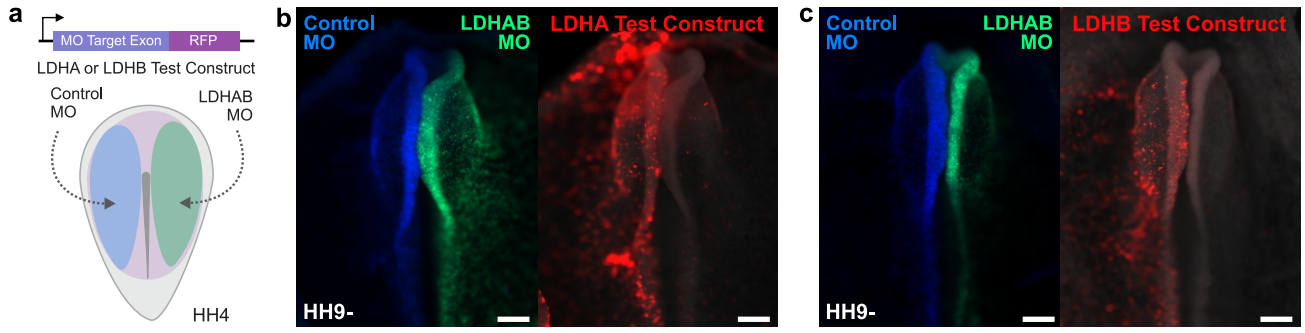
Supplementary Figure 4 – Quality control metrics for ATAC-seq performed on DMSO and (R)-GNE-140 treated NCC explant cultures.

(A) Scatterplot of read count from each DMSO ATAC-seq replicate alignment file at regions obtained after binning genome into 5 kb fragments (213335 bins). Magenta line is the line of best fit from regression analysis. (B) Overlaid histograms of read pair fragment size distribution for both DMSO ATAC-seq replicates. (C) Scatter plot of sequencing depth normalized ATAC-seq signal from each replicate at consensus DMSO peakset (40408 peaks). (D) Scatterplot of read count from each (R)-GNE-140 ATAC-seq replicate alignment file at regions obtained after binning genome into 5 kb fragments (213335 bins). (E) Overlaid histograms of read pair fragment size distribution for both (R)-GNE-140 ATAC-seq replicates. (F) Scatter plot of sequencing depth normalized ATAC-seq signal from each replicate at consensus DMSO peakset (4048 peaks). (G) Principal Component Analysis (PCA) plot showing replicates of each sample (DMSO and (R)-GNE-140). Principal component #1, accounting for most of the variance, separates the samples by treatment (dashed gray lines). (H) Profile plots showing enrichment of ATAC-seq signal at TSS for both replicates of each sample. (I) Scatterplot of read count (averaged between replicates) for DMSO and NF ATAC-seq samples at 5 kb genomic bins. (J) Genome browser tracks showing ATAC-seq peaks for explant (DMSO) and NF samples at the SNAI2 and SOX10 loci. RefSeq gene annotation tracks are used to visualize genes in genome browser panels. Non-curated non-coding RNA annotations are not displayed.



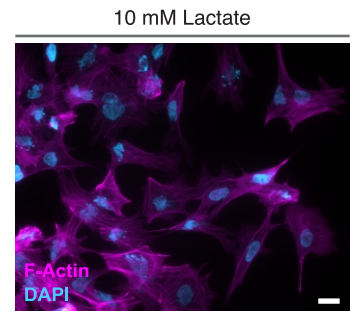
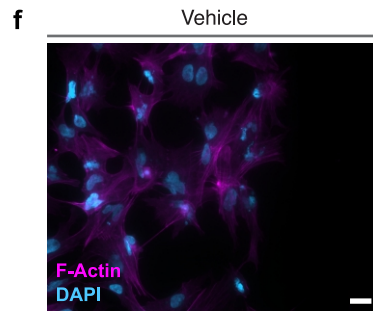
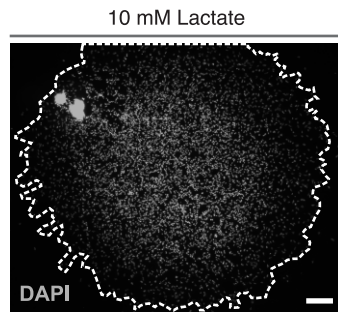
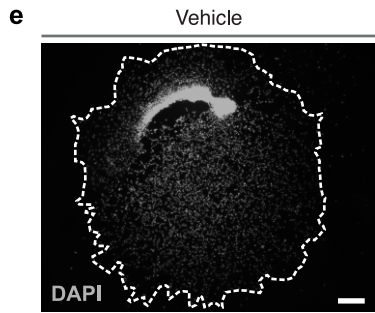
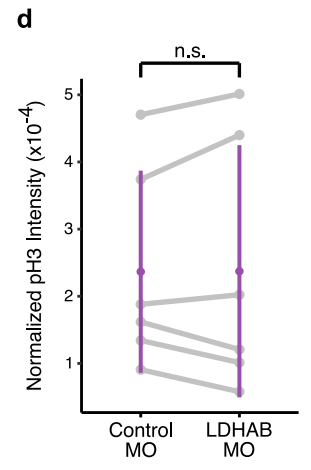
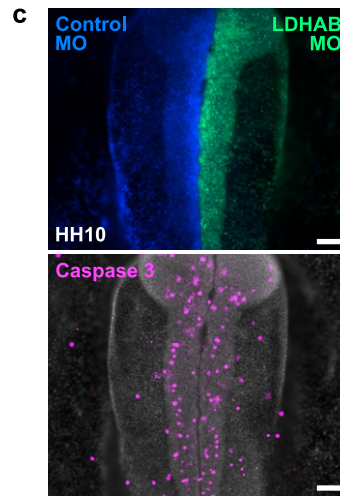
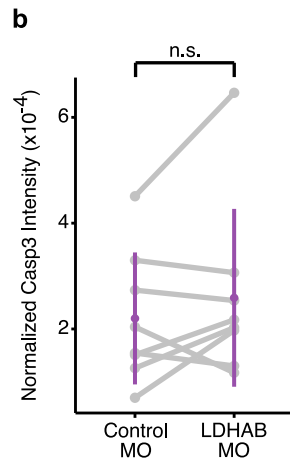
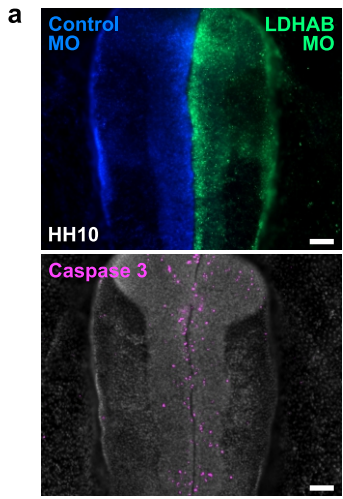
Supplementary Figure 5 – Quality control metrics for PanKla and H3K27ac CUT&RUNs performed on PSM cells.

(A) Scatterplot of read count from each PanKla replicate CUT&RUN alignment file at regions obtained after binning the genome into 5kb fragments (213312 bins). Magenta line is the line of best fit from regression analysis. (B) Overlaid histograms of read pair fragment size distribution for both PSM PanKla CUT&RUN replicates. (C) PCA plot comparing PanKla CUT&RUNs performed in NCCs (**Supplementary Figure 1A-1D**) and PSM cells. Principal component #1, accounting for most of the variance, separates the samples by cell type (dashed gray lines). (D) Scatterplot of read count from each H3K27ac replicate CUT&RUN alignment file at regions obtained after binning the genome into 5kb fragments (213312 bins). Magenta line is the line of best fit from regression analysis. (E) Overlaid histograms of read pair fragment size distribution for both PSM H3K27ac CUT&RUN replicates. (F) PCA plot comparing H3K27ac CUT&RUNs from NCCs and ones performed on PSM cells. Principal component #1, accounting for most of the variance, separates the samples by cell type (dashed gray lines). (G) Genome browser tracks showing PanKla CUT&RUN for NC and PSM cells as well as H3K27ac CUT&RUN for PSM cells at PSM-specific loci (FGF8, TBXT, and MSGN1).



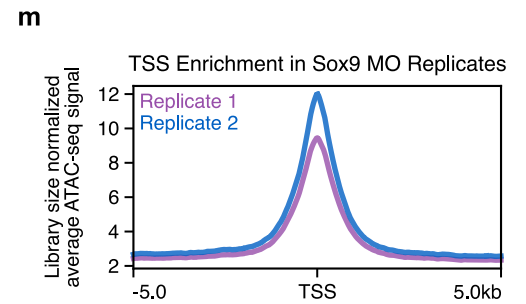
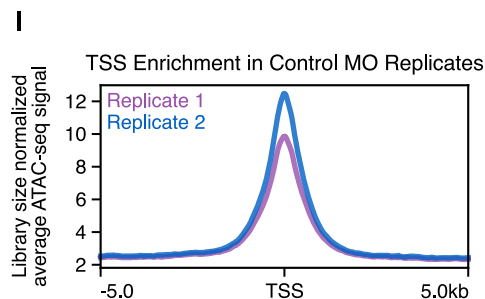
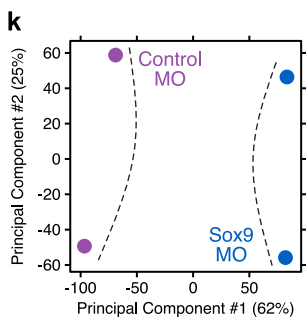
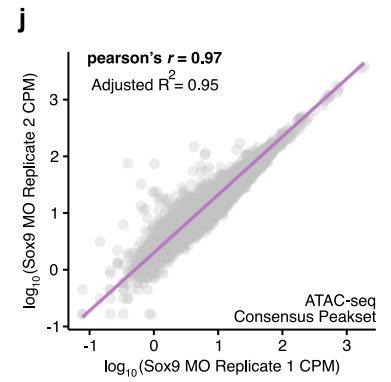
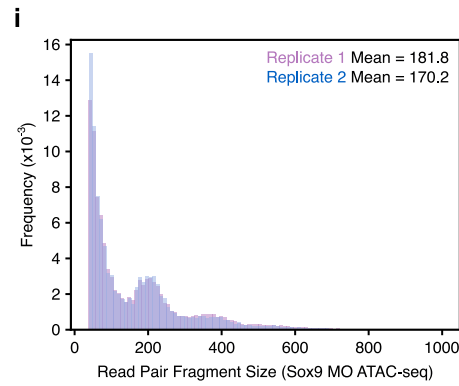
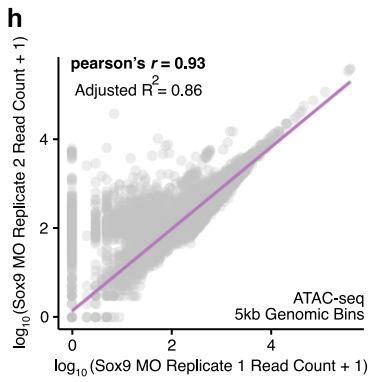
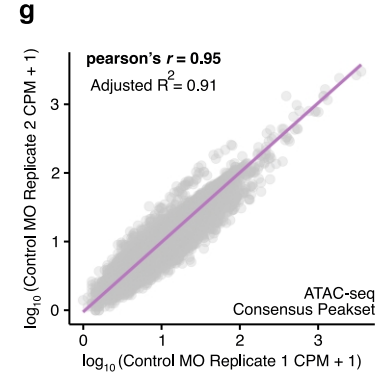
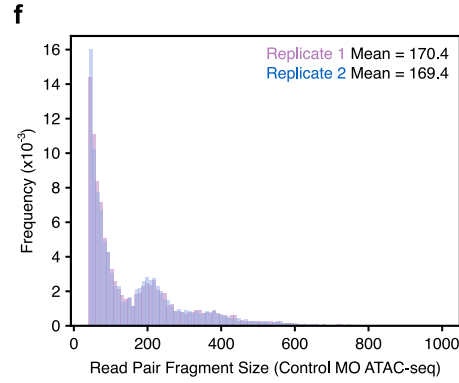
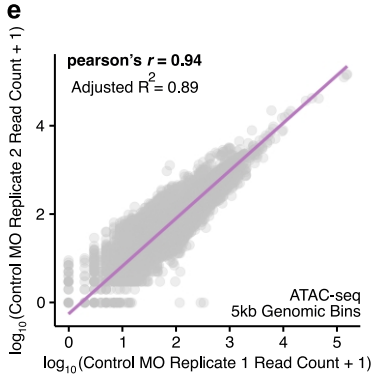
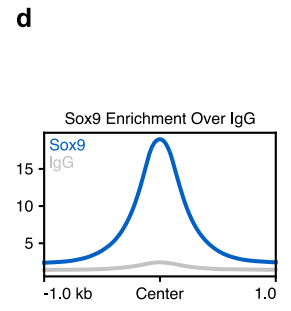
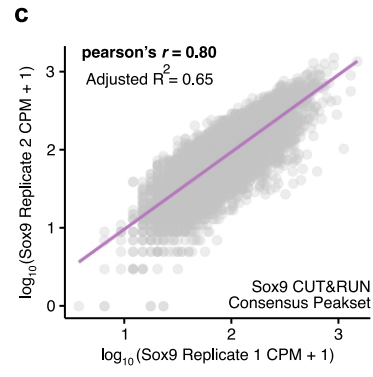
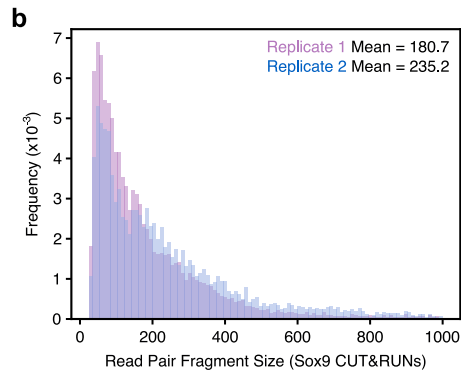
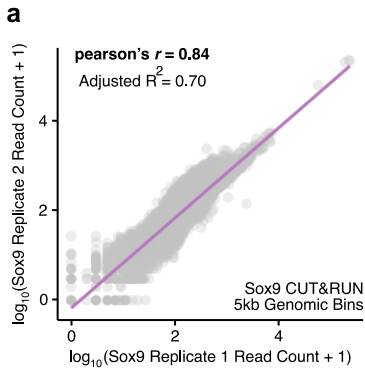
Supplementary Figure 6 – LDHA/B knockdown validation and flow cytometry gating strategy for lactylation level quantification in LDHA/B morphant and control HH9 embryonic head cells.

(A) Diagram depicting experimental strategy for testing the knock-down efficiency of LDHA and LDHB MOs. Embryos are injected one side with LDHA or LDHB test construct mixed with LDHA/B MO mix and on the other side with the same test construct mixed with the Control MO. (B) Image of bilaterally transfected HH9 embryo showing loss of RFP expression from the LDHA test construct on the LDHA/B MO transfected side (4/4 embryos display the similar loss of RFP expression). Scale bars represent 200 μm . (C) Image of bilaterally transfected HH9 embryo showing loss of RFP expression from the LDHB test construct on the LDHA/B MO transfected side (4/4 embryos display the similar loss of RFP expression). Scale bars represent 200 μm . (D-F) Contour plots showing the relative density of events in subsequent gating steps for cell samples stained only with secondary antibody (Alexa647). Gates are displayed as colored lines and the percentage/number of events in the gate is shown. Fluorescent intensity gates (F) are used to define the boundaries of the FITC population. (G-I) Contour plots showing the relative density of events in subsequent gating steps for FITC control MO cell samples stained for PanKla (Alexa647-A). Gates are displayed as colored lines and the percentage/number of events in the gate is displayed. The PanKla levels of cells in the blue gate (I) were quantified in FITC control and LDHAB MO samples. (J) Histogram of lactylation levels (Alexa647-A) for cells in the blue gate (F) for FITC control MO (blue, top) and LDHAB MO samples (purple, bottom). (K) Diagram depicting experimental strategy for quantifying the effects of LDHA/B MO treatment on lactylation levels. Each embryo was transfected with FITC control and LDHA/B MOs at HH4 and allowed to develop until HH9. Embryonic heads were bisected, collected, dissociated, and subjected to cell-suspension staining for PanKla. The cells were then analyzed on an BD FACSCelesta.



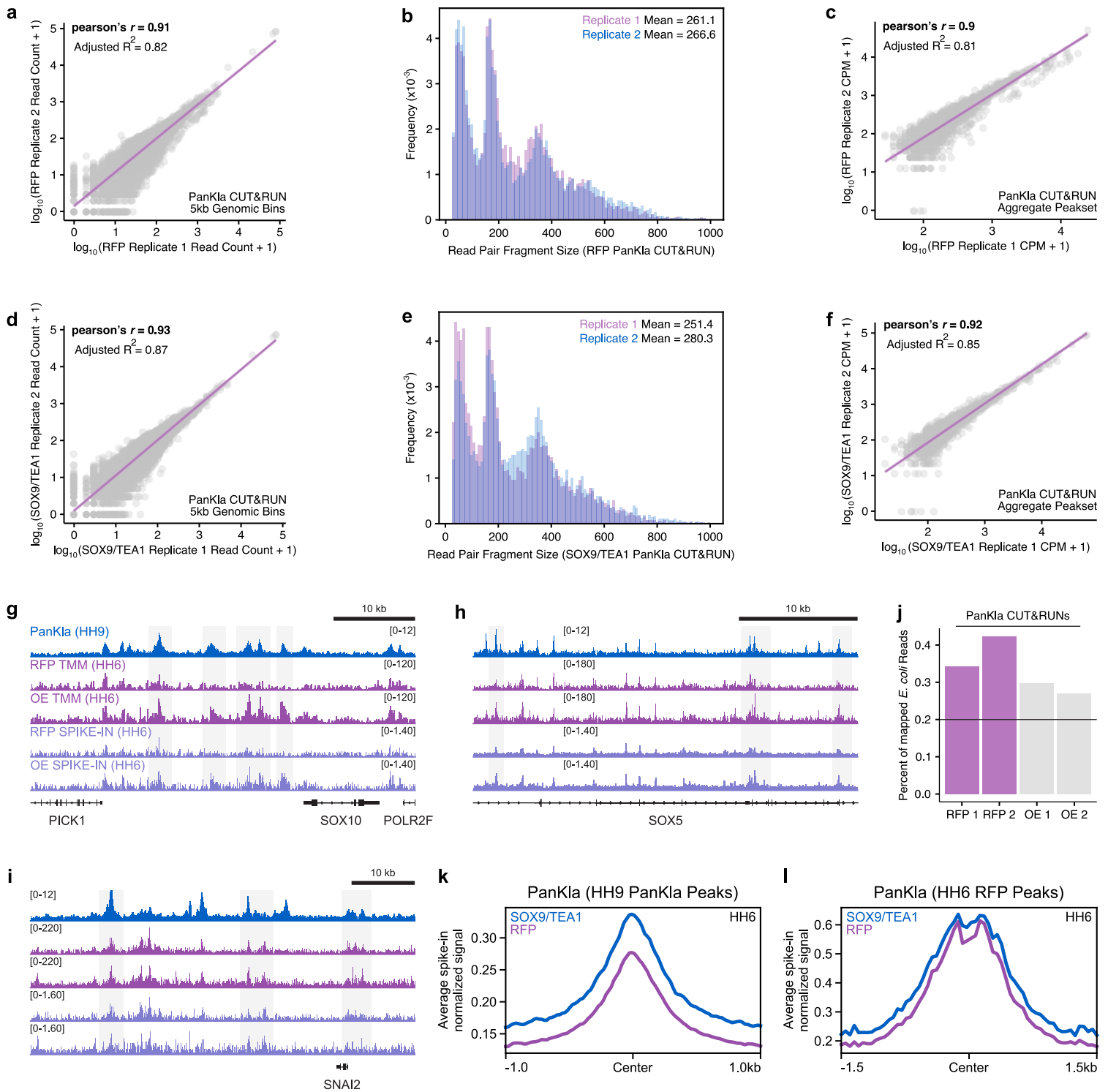
Supplementary Figure 7 – Control experiments for LDHA/B MO and lactate treatments.

(A) IF staining for Caspase 3 on embryo transfected with Control and LDHA/B MOs. Scale bars represent 100 μm . (B) Paired stripchart showing the quantification of Casp3 fluorescence intensity (normalized by area of measurement) in the Control and LDHA/B MO transfected sides of embryos. Purple bars represent standard deviation. For the analysis, n.s. p-value > 0.05 (p-value = 0.4609375), Wilcoxon signed rank test (n = 8 biological replicates). (C) IF staining for phosphor Histone H3 on embryo transfected with Control and LDHA/B MOs. Scale bars represent 100 μm . (D) Paired stripchart showing the quantification of pH3 fluorescence intensity (normalized by area of measurement) in the Control and LDHA/B MO transfected sides of embryos. Purple bars represent standard deviation. For the analysis, n.s. p-value > 0.05 (p-value = 0.84375), Wilcoxon signed rank test (n = 6 biological replicates). (E) Representative images showing whole explants in the vehicle control and 10 mM sodium lactate conditions used for analysis in Figure 4K. Scale bars represent 200 μm . (F) Higher magnification images of vehicle and sodium lactate treated cells stained for F-Actin and DAPI to show cellular morphology. Scale bars represent 20 μm .



Supplementary Figure 8 – Quality control metrics for SOX9 CUT&RUN and SOX9/Control MO ATAC-seq samples.

(A) Scatterplot of read count from each SOX9 replicate CUT&RUN alignment file at regions obtained after binning the genome into 5kb fragments (213311 bins). Magenta line is the line of best fit from regression analysis. (B) Overlaid histograms of read pair fragment size distribution for both SOX9 CUT&RUN replicates. (C) Scatter plot of sequencing depth normalized SOX9 signal from each replicate at consensus SOX9 peakset (9699 peaks). (D) Profile plot showing cumulative SOX9 and IgG signal at SOX9 consensus peakset. SOX9 signal displayed as average between replicates. (E) Scatterplot of read count from each Control MO ATAC-seq replicate alignment file at regions obtained after binning genome into 5 kb fragments (213367 bins). Magenta line is the line of best fit from regression analysis. (F) Overlaid histograms of read pair fragment size distribution for both Control MO ATAC-seq replicates. (G) Scatter plot of sequencing depth normalized ATAC-seq signal from each replicate at consensus Control MO peakset (73479 peaks). (H) Scatterplot of read count from each SOX9 MO ATAC-seq replicate alignment file at regions obtained after binning genome into 5 kb fragments (213367 bins). Magenta line is the line of best fit from regression analysis. (I) Overlaid histograms of read pair fragment size distribution for both SOX9 MO ATAC-seq replicates. (J) Scatter plot of sequencing depth normalized ATAC-seq signal from each replicate at consensus SOX9 MO peakset (84529 peaks). (K) Principal Component Analysis (PCA) plot showing replicates of each sample (Control and SOX9 MO). Principal component #1, accounting for most of the variance, separates the samples by treatment (dashed gray lines). (L – M) Profile plots showing enrichment of ATAC-seq signal at TSS for both replicates of each sample.



Supplementary Figure 9 – Quality control metrics for SOX9/TEA1-VPR over-expression CUT&RUN experiment.

(A) Scatterplot of read count from each PanKla CUT&RUN performed on pCI-H2B-RFP (Control) replicate samples (transfected HH6 embryos). Read count computed for each alignment file at regions obtained after binning the genome into 5kb fragments (213313 bins). Magenta line is the line of best fit from regression analysis. (B) Overlaid histograms of read pair fragment size distribution for PanKla CUT&RUNs performed on pCI-H2B-RFP replicate samples. (C) Scatter plot of sequencing depth normalized PanKla signal from each pCI-H2B-RFP replicate at aggregate PanKla peakset from control (RFP) and SOX9/TEA1-VPR over-expression (OE) peaksets (2188 peaks). (D) Scatterplot of read count from each PanKla CUT&RUN performed on OE replicate samples (transfected HH6 embryos). Read count computed for each alignment file at regions obtained after binning the genome into 5kb fragments (213313 bins). Magenta line is the line of best fit from regression analysis. (E) Overlaid histograms of read pair fragment size distribution for PanKla CUT&RUNs performed on OE replicate samples. (F) Scatter plot of sequencing depth normalized PanKla signal from each OE replicate at aggregate PanKla peakset from RFP OE peaksets (2188 peaks). (G - I) Genome browser tracks showing the average (between replicates) normalized (spike-in and TMM) signal for RFP and OE samples at the SOX10, SOX5, and SNAI2 loci. Tracks are arranged in the same order as panel G. (J) Barplot of the percent of reads from the fastq files associated with the experimental samples that mapped to the *E. coli* genome. These values were used to calculate spike-in normalization of experimental samples as described by Skene et al., 2018⁴ (see Methods section). The fraction of *E. coli* reads in these samples is consistent with previous reports using CUT&RUN assays⁴. (K) Profile plot showing the average cumulative spike-in normalized HH6 PanKla CUT&RUN signal of RFP (magenta) and SOX9+TEA1-VPR (purple) samples at HH9 PanKla CUT&RUN consensus peakset. (L) Profile plot showing the average cumulative spike-in normalized HH6 PanKla CUT&RUN signal of RFP (magenta) and SOX9+TEA1-VPR (purple) samples at HH6 PanKla CUT&RUN RFP aggregate peakset (2188 peaks). RefSeq gene annotation tracks are used to visualize genes in genome browser panels. Non-curated non-coding RNA annotations are not displayed.